A novel, non-metallic graphitic carbon nitride catalyst for acetylene hydrochlorination

CrossMark

Xiaoyan Li [a], Yang Wang [a], Lihua Kang [a,b], Mingyuan Zhu [a,b,*], Bin Dai [a,b,*]

[a] School of Chemistry and Chemical Engineering of Shihezi University, Shihezi, Xinjiang 832000, PR China
[b] Key Laboratory for Green Processing of Chemical Engineering of Xinjiang Bingtuan, Shihezi, Xinjiang 832000, PR China

A B S T R A C T

Graphitic carbon nitride (g-C_3N_4) was prepared using a simple method. Activated carbon (AC) was used to support the g-C_3N_4 catalyst. Catalytic evaluation indicated that the g-C_3N_4/AC catalyst had enhanced catalytic activity for acetylene hydrochlorination as a non-metallic catalyst when compared to AC. X-ray photoelectron spectra confirmed the presence of nitrogen and carbon species in the prepared g-C_3N_4/AC catalysts. Temperature-programed decomposition results indicated that hydrogen chloride was notably well adsorbed onto g-C_3N_4/AC catalysts. Theoretical calculations indicated that hydrogen chloride is adsorbed at the nitrogen atom and that acetylene is adsorbed at the carbon atom of g-C_3N_4. The transfer of a proton from the nitrogen atom to the chloroethenyl moiety is the rate-limiting step. The combination of activation of both reactants and facile product desorption makes g-C_3N_4 an interesting catalyst for acetylene hydrochlorination.

Crown Copyright © 2013 Published by Elsevier Inc. All rights reserved.

1. Introduction

Polyvinyl chloride (PVC) is the most widely used thermoplastic resin. This resin can be manufactured into hard products, which have a wide variety of applications, including pipes and fittings, doors, windows and packaging sheets [1,2]. The vinyl chloride monomer (VCM) is the monomer used to manufacture PVC. Depending on the energy structure of China, an important industrial route for manufacturing VCM is through acetylene hydrochlorination [3]. However, the $HgCl_2$ catalyst used for acetylene hydrochlorination is highly toxic and harmful to human health and the environment [4]. Therefore, research efforts have been undertaken to explore non-mercury catalysts for acetylene hydrochlorination.

There are many reports in the literature of metal chlorides, including Bi^{3+} [5], Pt^{2+} [6,7] and Pd^{2+} [8] chlorides, displaying considerable activity toward catalyzing the acetylene hydrochlorination. Hutchings [9,10] reported that Au-based catalysts were the optimal metal chloride catalysts for acetylene hydrochlorination. However, the Au-based catalyst is easily deactivated over the course of the reaction, which is attributed to the reduction of the active Au^{3+} species to metallic Au during acetylene hydrochlorination [11,12]. To improve the stability of Au-based catalysts, investigators

tried other metal additives. A bimetallic Au—Cu/C catalyst showed favorable catalytic activity and an acetylene conversion of 99.5% at 200 h [13]. In our previous study, the addition of La^{3+} to an Au^{3+} catalyst improved the stability of the Au catalyst and extended the catalyst lifetime [14]. Furthermore, an Au—Co catalyst can be used for 50 h without obvious deactivation [15]. As Au is expensive and scarce, exploitation of low-cost catalysts may be another development direction of acetylene hydrochlorination catalyst.

In recent years, nanocarbon-based materials have attracted much attention in catalysis, and it can be considered an emerging and conceptually new area of catalytic materials [16,17]. Graphitic carbon nitride (g-C_3N_4) has been widely used in many catalytic areas, and especially for oxygen reduction reactions (ORR). In the acetylene hydrochlorination, acetylene is the electron donor that adsorbs onto the catalytic active site [11], which is similar to O_2 adsorption in the ORR process. Therefore, we hypothesized that g-C_3N_4 might display catalytic activity in the acetylene hydrochlorination. The aim of these studies is to explore a novel non-mercury catalyst for acetylene hydrochlorination, which is much cheaper than previously reported Au and Ru-based catalysts. To the best of our knowledge, there are no reports of non-metallic catalysts for acetylene hydrochlorination with high conversions of acetylene. In this study, graphitic carbon nitride with N-rich porous carbon was prepared by a simple method using cyanamide as a precursor. The catalytic activity of the obtained catalyst was evaluated, and its reasonable activity was explained by a temperature-programed decomposition (TPD) experiment and theoretical calculations.

* Corresponding authors. Address: School of Chemistry and Chemical Engineering of Shihezi University, Shihezi, Xinjiang 832000, PR China. Fax: +86 993 2057210.
E-mail addresses: zhuminyuan@shzu.edu.cn (M. Zhu), daibin_tea@shzu.edu.cn (B. Dai).

2. Experimental

2.1. Materials

Activated carbon (neutral, coconut carbon, 40–60 mesh, the property of the carbon was shown in Table S1, Figs. S1 and S2 in Supporting Information), C_2H_2 (gas, 98%), HCl (gas, 99%), and cyanamide (CN—NH$_2$, 99%, Aldrich) were used in the present study.

2.2. Catalyst preparation

Dicyandiamine was transferred into a crucible and calcined at a rate of 2.3 K min^{-1} over 4 h to reach a temperature of 500 °C, which was held for another 4 h before the yellow sample was allowed to cool, yielding the g-C3N4 product [18].

The g-C$_3$N$_4$/AC catalysts were prepared using the AC as the carrier and cyanamide as precursor by an incipient wetness impregnation technique. About 0.2 g of a 50 wt.% cyanamide aqueous solutions and 5 mL distilled water were added dropwise to 1.0 g of AC powder, the mixture was stirred 12 h, and the resulting product was then dried at 30 °C for 24 h. The dried powder was calcined at 500 °C for 4 h in a N$_2$ atmosphere with a heating rate of 2.3 K min^{-1}, as described in the literature [19]. Using the same method, the amount of cyanamide species was varied from 0.2 g to 0.7 g while keeping the AC content constant, and the obtained samples were labeled as 1# g-C$_3$N$_4$/AC, 2# g-C$_3$N$_4$/AC, 3# g-C$_3$N$_4$/AC, 4# g-C$_3$N$_4$/AC, 5# g-C$_3$N$_4$/AC, and 6# g-C$_3$N$_4$/AC, respectively.

2.3. Catalyst characterization

Brunauer–Emmett–Teller (BET) surface area data were collected using a Micromeritics ASAP 2020 instrument by obtaining nitrogen adsorption isotherms at 77 K. X-ray diffraction (XRD) patterns at wide (10–90° in 2θ) angles were collected using a Bruker D8 advanced X-ray diffractometer with Cu Kα irradiation (λ = 1.5406 Å) at 40 kV and 40 mA. Transmission electron microscopy (TEM) was performed using a JEM 2010 electron microscope at an accelerating voltage of 200 kV to examine the sample morphologies. X-ray photoelectron spectroscopy (XPS) was performed by an Axis Ultra spectrometer with a monochromatized Al Kα X-ray as the excitation source (225 W). Temperature-programed decomposition (TPD) was determined using a Micromeritic ASAP 2720 instrument over a temperature ramp of 40–650 °C, ramp rate of 10 °C min^{-1}, flow of 45 mL min^{-1}, and final temperature of 650 °C. Thermogravimetric analysis (TGA) of samples was conducted on the TGDSC simultaneous thermal analyzer (NETZSCH STA 449F3 Jupiter1, Germany). About 7 mg of sample was used and heated to 900 °C under the oxygen atmosphere, flow rate of 30 mL min^{-1}, and heating rate of 10 °C min^{-1}. Energy dispersive X-ray (EDX) and Raman spectra analyses were given in Supporting Information.

The catalytic performance tests were evaluated in a fixed-bed micro-reactor (i.d. 10 mm). The temperature of the reactor was regulated by a CKW-1100 temperature controller produced by (Beijing, China). Nitrogen was used to purge the reactor containing catalyst (0.80 g) to remove water and air before running the reaction. Hydrogen chloride gas was passed through the reactor at a flow rate of 20 mL min^{-1} to activate the catalyst. Acetylene (2.0 mL min^{-1}) and hydrogen chloride (1.7 mL min^{-1}) were fed through the heated reactor at a gas hourly space velocity (GHSV) of 50 h^{-1} and a reaction temperature of 180 °C. The reaction products were analyzed by gas chromatography (GC-2014C).

2.4. Computational details

DFT calculations were performed using the hybrid B3LYP [20,21] function, as implemented in the Gaussian 09 computer program package [22]. The standard 6-311G++** basis set was used for H, C, N and C(l) atoms. Atomic charges were calculated using the Mulliken type. The geometries of all structures involved in the mechanism were optimized fully without any restrictions. The frequencies of all geometries were calculated at the same level to identify the nature of the stationary points and obtain the zero-point-energy (ZPE) corrections. All stationary points were characterized as minima (no imaginary frequencies) or transition states (one imaginary frequency) by a Hessian calculation. Intrinsic reaction coordinate (IRC) calculations [23,24] were used to determine if each transition state linked the correct product with each reactant.

3. Results and discussion

XRD was performed to investigate the structure of the g-C$_3$N$_4$/AC catalysts, and the results are shown in Fig. 1. Two obvious diffraction peaks were observed for g-C$_3$N$_4$ (Fig. 1a) at 13.13° and 27.19°. The strongest peak at 27.19°, the (0 0 2) peak, is a characteristic interplanar stacking peak of aromatic systems, and the peak at 13.13° is typical of more oriented melons [25]. Two obvious diffraction peaks in the pattern of the AC support appear at 23.16° and 43.84°, corresponding to the (0 0 2) and (1 0 1) planes, respectively [26]. The broad peaks appearing from 18.16° to 27.76° for the g-C$_3$N$_4$/AC catalysts are clearly attributable to the diffraction of AC and the presence of g-C$_3$N$_4$, which is well dispersed on the support surface. Moreover, the broad peaks observed for the g-C$_3$N$_4$/AC catalysts has a positive shift when the amount of cyanamide precursor used was increased from 0.2 to 0.7 g.

Experiments to determine the specific surface areas and total pore volumes were performed to investigate the physical structures of the prepared g-C$_3$N$_4$/AC catalysts. The textural parameters of AC and the 1# g-C$_3$N$_4$/AC, 2# g-C$_3$N$_4$/AC, 3# g-C$_3$N$_4$/AC, 4# g-C$_3$N$_4$/AC, 5# g-C$_3$N$_4$/AC, and 6# g-C$_3$N$_4$/AC catalysts are also given in Table 1. The specific surface area of the g-C$_3$N$_4$/AC catalysts decreased from 1138.2 m^2 g^{-1} to 74.2 m^2 g^{-1} and the specific pore volume decreased from 0.64 cm^3 g^{-1} to 0.48 cm^3 g^{-1}, as the precursor cyanamide content increased from 0.2 g to 0.7 g. These results suggest that the AC pores are filled or blocked, and thus the BET surface area and the total pore volume decreased.

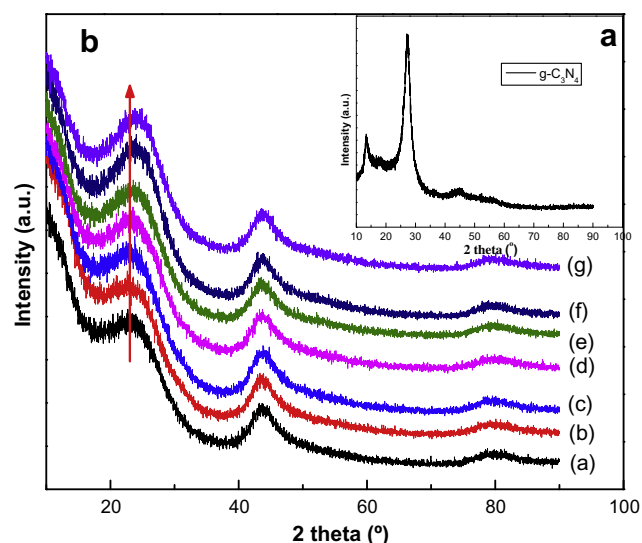The structure and morphology of g-C$_3$N$_4$, AC, and 5# g-C$_3$N$_4$/AC catalysts can be clearly observed in the TEM image (Fig. 2). The

Fig. 1. XRD patterns of: (a) AC, (b) 1# g-C$_3$N$_4$/AC, (c) 2# g-C$_3$N$_4$/AC, (d) 3# g-C$_3$N$_4$/AC, (e) 4# g-C$_3$N$_4$/AC, (f) 5# g-C$_3$N$_4$/AC and (g) 6# g-C$_3$N$_4$/AC.